



Benchmarking: An International Journal

Concurrent design of nanofluid for x-abilities using MADM approach

Jyoti Prakash Vishnu P. Agrawal

Article information:

To cite this document:

Jyoti Prakash Vishnu P. Agrawal , (2016),"Concurrent design of nanofluid for x-abilities using MADM approach", Benchmarking: An International Journal, Vol. 23 Iss 5 pp. 1286 - 1311

Permanent link to this document:

<http://dx.doi.org/10.1108/BIJ-07-2014-0062>

Downloaded on: 14 November 2016, At: 01:16 (PT)

References: this document contains references to 18 other documents.

To copy this document: permissions@emeraldinsight.com

The fulltext of this document has been downloaded 51 times since 2016*

Users who downloaded this article also downloaded:

(2016),"Benchmarking the competitiveness of the ASEAN 5 equity markets: An application of Porter's diamond model", Benchmarking: An International Journal, Vol. 23 Iss 5 pp. 1312-1340 <http://dx.doi.org/10.1108/BIJ-05-2014-0047>

(2016),"Benchmarking operating room departments in the Netherlands: Evaluation of a benchmarking collaborative between eight university medical centres", Benchmarking: An International Journal, Vol. 23 Iss 5 pp. 1171-1192 <http://dx.doi.org/10.1108/BIJ-04-2014-0035>

Access to this document was granted through an Emerald subscription provided by emerald-srm:563821 []

For Authors

If you would like to write for this, or any other Emerald publication, then please use our Emerald for Authors service information about how to choose which publication to write for and submission guidelines are available for all. Please visit www.emeraldinsight.com/authors for more information.

About Emerald www.emeraldinsight.com

Emerald is a global publisher linking research and practice to the benefit of society. The company manages a portfolio of more than 290 journals and over 2,350 books and book series volumes, as well as providing an extensive range of online products and additional customer resources and services.

Emerald is both COUNTER 4 and TRANSFER compliant. The organization is a partner of the Committee on Publication Ethics (COPE) and also works with Portico and the LOCKSS initiative for digital archive preservation.

*Related content and download information correct at time of download.

Concurrent design of nanofluid for x-abilities using MADM approach

Jyoti Prakash and Vishnu P. Agrawal

Department of Mechanical Engineering, Thapar University, Patiala, India

1286

Received 4 July 2014
Revised 27 August 2015
Accepted 5 September 2015

Abstract

Purpose – Multiple attribute decision making (MADM) is a conceptual agenda used for evaluation and selection of optimal nanofluid to assure best performance of heat exchanger. Most of the studies focus on nanofluids focus on individual ability at one time. Relatively, not even a single study is available for selection of nanofluid for heat exchanger using concurrent design and MADM approach. The purpose of this paper is to propose a concurrent design methodology using MADM approach to assist improved design of heat exchanger concurrently for all the x-abilities in an integrated manner.

Design/methodology/approach – A combined methodology of applying MADM approach using concurrent design for x-abilities is called CE-MADM approach. Implementation of nanofluid to improve thermal performance of heat exchanger entails thorough evaluation of nanofluids in various x-abilities (performance, maintenance, thermophysical properties and modelisation) to make exhaustive management decision. Sensitivity analysis is also proposed to study the behaviour of height of variation of density, heat capacity, thermal expansion and thermal conductivity with varying particle volume fraction and variation of relative closeness of available alternates from ideally best possible solution.

Findings – MADM approach considering various x-abilities concurrently provide an approach for relative ranking of available nanofluids for optimum performance. Fishbone diagrams of all x-abilities are constructed to identify all the attributes and converge large number of attributes into single numerical index that are concurrently responsible for the cause thus saving time for easy evaluation, comparison and ranking by decision makers. Sensitivity analysis to demonstration height of variation of pertinent attributes with varying particle volume fraction. A MATLAB programming is established to execute calculations involved in the procedure.

Originality/value – This paper comprises a predictable and effective mathematical approach to improve design of heat exchanger with nanofluid bearing in mind all the required x-abilities concurrently. This combined approach of CE-MADM is never applied before in the field of nanofluid to predict best possible results in feasible conditions considering all the x-abilities. Sensitivity analysis is also presented from the assumed mathematical equations of thermophysical properties.

Keywords Nanofluid, CE-MADM, Concurrent design, X-abilities

Paper type Conceptual paper

Introduction

Growing demands of efficient heat transfer for industrial and thermal engineering applications has diverted significant attention towards research and practices on nanofluid characteristics and applications (Wong and De Leon, 2010; Taylor *et al.*, 2012; Yu and Xie (2012)) that potentially leads to better heat transfer performance. In the field of thermal heat transfer equipment's, low thermal conductivity of conventionally used heat transfer fluid was a serious constraint in enhancing the performance and compactness of engineering apparatus. This requires amendments in the design of heat exchanger or improvement in the fluid participating for heat transfer for varieties of different applications to improve performance. One of the idea of increasing heat transfer rate by increasing relative surface area that actively participate in heat transfer. On the path of increasing surface area, growth of nanotechnology has observed a beginning of new generation of heat transfer fluid known as nanofluid.



Usage of fins, elongated tubes in heat exchanger, wavy channel (Ahmed *et al.*, 2012; Sui *et al.*, 2011) and blocks (Bhave *et al.*, 2006; Heidary and Kermani, 2012) in passage of flow are also based on the fact of increasing relative surface area for better heat transfer performance. The concept of increasing heat transfer performance by increasing surface area have been studied numerically and experimentally by many researchers by using nanofluids (Choi, 1995; Ahmed *et al.*, 2012; Maxwell, 1881; Hamilton and Crosser, 1962; Yu and Choi, 2003; Eisher *et al.*, 2011; Peyghambarzadeh *et al.*, 2011) or by altering geometry of walls (Ahmed *et al.*, 2012; Sui *et al.*, 2011; Mahmoodi and Hashemi, 2012; Heidary and Kermani, 2012).

Nanofluid is a two phase heat transfer fluid consist of a base fluid with nano-sized particles uniformly suspended in it and behaves like a single phase fluid. It work on the principle that thermal conductivity of metallic solid is extensively higher than fluid, as a consequence fluid comprising suspended solid particles are likely to exhibit comparatively higher thermal conductivity than that of the conventional fluid. Choi (1995), presented first report on two phase fluid with the nano size of particles, and named it as nanofluid. And with continuous innovation till now these nanofluids are now available with new ideas and challenges to reduce size of thermal equipment's with vastly different enhanced capabilities working with high potential (Wong and De Leon, 2010; Taylor *et al.*, 2012; Yu and Xie (2012)). Emerging developments in applications of nanofluids make it possible to cast small and much efficient devices (Eisher *et al.*, 2011). Singh and Agrawal (2012) proposed a methodology for combining all the design aspects of x-abilities together in concurrent design methodology using multiple attribute decision making (MADM) approach to design Nanoactuator. The basic need for upcoming heat transfer equipment is high thermal performance with reduced size. One of the recent methods to increase thermal performance of heat exchanger include usage of nanofluid as a heat transfer medium introducing new abilities or potential in various applications. These abilities are called x-abilities. Designing heat exchanger for improved performance, resilience, maintenance and modelisation necessitate re-examining of design constraints for abilities previously considered. This designing procedure for a nanofluid in heat exchanger for all the x-abilities concurrently is called concurrent engineering. Most of these studies focus on individual ability at one time. Relatively, not even a single study is available for selection of nanofluid for heat exchanger using concurrent design and MADM approach. A combined methodology of applying MADM approach using concurrent design for x-abilities is suggested. This combined methodology is called CE-MADM approach. In the same context this paper includes a conventional and effective mathematical methodology to improve design of heat exchanger working with nanofluid considering all the required x-abilities concurrently. Different attributes affecting x-abilities are analysed and represented in fishbone diagram are observed by literature survey on the relevant themes. Ahmed *et al.* (2012) examined numerical attempt on nanofluid in heat exchanger by amending geometry of passage of flow, i.e. wavy channel and noticed that increase in nanoparticle volume fraction and wavy amplitude cause increase in friction coefficient for all values of Reynolds number and further it was analysed that enhancement in heat transfer performance depends on particle volume fraction, amplitude and Reynolds number rather than wave length of the wave wall by using finite difference method.

To study effective thermal conductivity of heterogeneous medium Maxwell (1881), Hamilton and Crosser (1962), Yu and Choi (2003) presented three important standard models to measure and study the attributes affecting thermal conductivity. Maxwell (1881) prepared a two phase heterogeneous model for effective thermal

conductivity of the suspension of micro-sized particles, K_{eff} :

$$K_{eff} = \frac{2K_f + K_p + 2\phi(K_p - K_f)}{2K_f + K_p - \phi(K_p - K_f)} K_f \quad (1)$$

Hamilton and Crosser (1962) modified the former expression of effective thermal conductivity of suspension formulated by Maxwell (1881) with the introduction of new attribute shape factor (n):

$$K_{eff} = \frac{K_p + (n-1)K_f - (n-1)\phi(K_f - K_p)}{K_p + (n-1)K_f + \phi(K_f - K_p)} K_f \quad (2)$$

where $n = 3/\psi$ for sphere $n = 3$, for cylinder $n = 6$.

Yu and Choi (2003) presented the role of nanolayer generated on the surface of nanoparticle in enhancing thermal conductivity of the suspension and proposed a renovated Maxwell model.

Thermal conductivity of equivalent particle (nanoparticle with nanolayer) is given as:

$$K_{eq} = \frac{[2(1-\gamma) + (1+\beta)^3(1+2\gamma)]\gamma}{-(1-\gamma) + (1+\beta)^3(1+2\gamma)} K_p \quad (3)$$

Assume a spherical nanoparticle of radius r enclosed by a thin nanolayer of thickness h and thermal conductivity K_{layer} . This K_{layer} is higher than thermal conductivity of base fluid K_f but lower than thermal conductivity of particle K_p :

$$\gamma = \frac{K_{layer}}{K_p},$$

and:

$$\beta = \frac{h}{r}$$

Effective thermal conductivity " K_{eff} " is:

$$K_{eff} = \frac{K_{eq} + 2K_f + 2(K_{eq} - K_f)(1+\beta)^3\phi}{K_{eq} + 2K_f - (K_{eq} - K_f)(1+\beta)^3\phi} K_f \quad (4)$$

Wong and De Leon (2010), Taylor *et al.* (2012) and Yu and Xie (2012) presented a broad range of current and future applications of nanofluid in biomedical engineering, bioscience field and various thermal heat transfer-related fields so that proper predictions of nanofluid abilities can be made and nanofluids can be applied as predicted. Eisher *et al.* (2011) prepared characterisation of SiO₂ – water nanofluid for particle size of 22 nm and measured thermophysical properties of nanofluid namely, specific heat capacity, density, thermal conductivity and dynamic viscosity at particle volume fraction of 0, 5, 16 and 31 per cent experimentally and theoretically from the standard correlations being used. He used Maxwell modified expression for thermal conductivity that was formulated by Hamilton and Crosser (1962) represented in Equation (2) as a standard correlations for effective thermal conductivity of nanofluid:

$$\rho_{nf} = (1-\phi)\rho_f + \phi\rho_p \quad (5)$$

$$(\rho C_p)_{nf} = (1-\phi)(\rho C_p)_f + \phi(\rho C_p)_p \quad (6)$$

$$\beta_{nf} = (1-\phi)\beta_f + \phi\beta_p \quad (7)$$

$$\mu_{nf} = \frac{\mu_f}{(1-\phi)^{2.5}} \quad (8)$$

They calculated Nusselt number experimentally and theoretically and demonstrated a deviation of less than 10 per cent between the experimental and predicted values as a consequence, he validated that these correlations may be used to measure thermophysical properties of nanofluid. Same validated standard correlations that are used by Eisher *et al.* (2011) are used in this paper to predict specifications of thermophysical properties. Sui *et al.* (2011) investigated on experimental setup to study flow friction and heat transfer on wavy microchannel comprising ten identical wavy units with rectangular cross-section and compared measured values of overall Nusselt number and friction factor for microchannel arrangement and straight base line channel having same cross-section and length of path. As a result he recommended use of microchannel heat sink based on wavy channel over straight channels. Similarly, Mahmoodi and Hashemi (2012) amended the shape of channel in C-shape enclosure to study the behaviour of nanofluid. Zoubida Haddad *et al.* (2012), Eastman *et al.* (2004) and Koblinski *et al.* (2002) predicted and defined four probable mechanisms to explain the reasons for anomalous increase of thermal conductivity in nanofluids that are nanoparticles Brownian motion, molecular-level layering of liquid at the liquid-particle interface known as nanolayer, ballistic heat transport in nanoparticles, i.e. lattice vibrations of phonons and clustering of nanoparticles. Peyghambarzadeh *et al.* (2011) performed an experiment to investigate enhancement in heat transfer performance of water and EG-based nanofluids as a new coolant in car radiator. The nanofluid used for experiment with different volume fraction of Al_2O_3 ranging from 0.1-1 per cent and with altering inlet temperature (35, 45 and 500°C for water-based nanofluid and 45, 50 and 600°C for EG-based nanofluid). He recorded 40 per cent increase in Nusselt number as compared to pure water or EG at 1 per cent volume fraction of Al_2O_3 nanoparticle. Heidary and Kermani (2012) analysed the fluid flow at temperature T_{in} and volume fraction of 10 per cent in a channel with three blocks attached at hot bottom wall at temperature T_w ($T_w > T_{in}$) and observed enhancement in rate of heat transfer and Reynolds number with enhancement in average Nusselt number. There are large number of attributes that must be considered in designing heat exchanger with nanofluid related to manufacturing, production process, supplying, installing, operating, maintenance and disposal. Here a small attempt is made to propose a CE-MADM methodology for concurrent design of heat exchanger with nanofluid as a heat transfer medium for x-abilities. This practice ensures that optimally nominated alternate is nearest to positive ideal solution and farthest away from negative ideal solution as possible.

Design methodology for x-abilities

Combined approach of CE-MADM methodology permits more rapidly design flow with concurrent/simultaneous consideration of design goals and constraints merging experts from different fields into a group. This is a systematic approach that simultaneously consider all the design objectives.

Design flow

Design flow is prepared to reveal the suggested concurrent design methodology for a heat exchanger in Figure 1. Design flow procedure include systematic sequence of steps

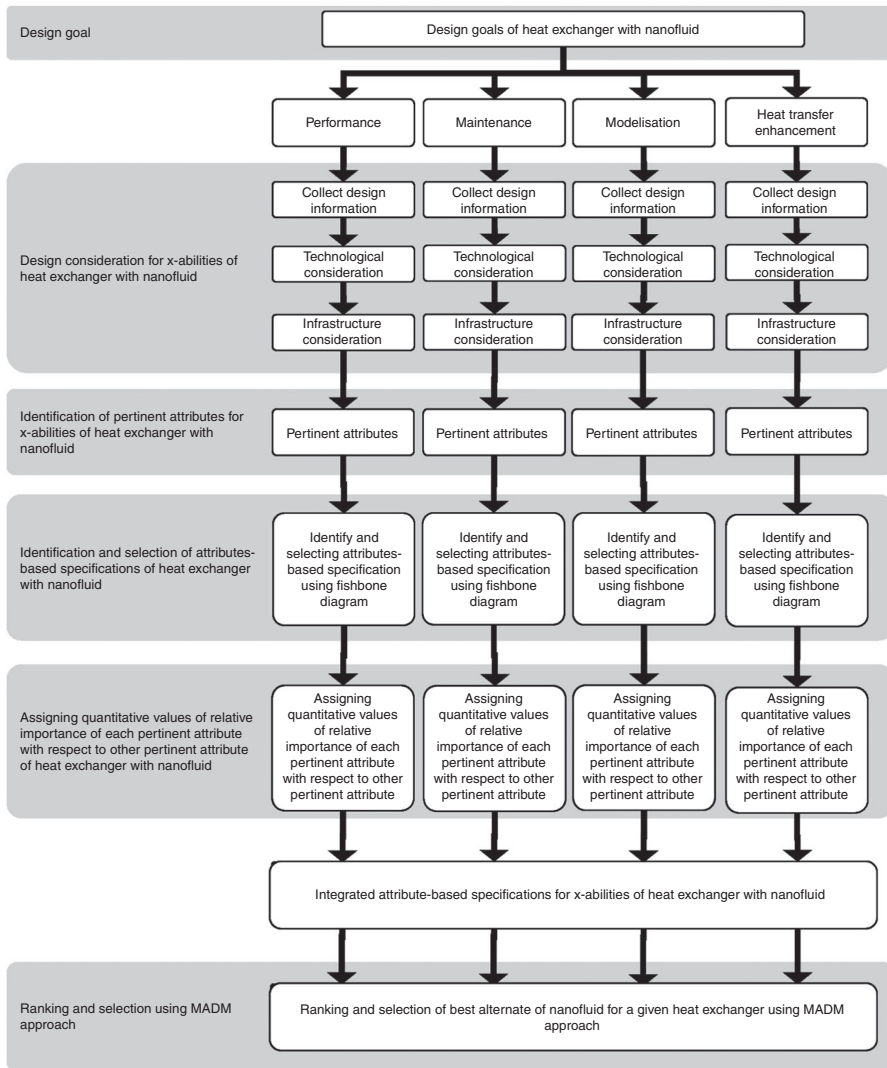


Figure 1.
Design flow chart
for heat exchanger
with nanofluid

considering all alternates and their pertinent attributes simultaneously. This procedure initiates with specifying heat exchanger design goals that comprise objective and requirements from manufacturer, user and maintenance unit. For example, if the application demands best possible performance of heat exchanger with nanofluid as a heat transfer fluid then thorough understanding of inherit attributes, infrastructure standards, properties, specifications, constraints, forte and flaws of system and application is required. Fishbone/Ishikawa/cause and effect diagram is developed to design goals and to identify inherit attributes that directly or indirectly affects our objective. Various applications entail x-abilities with varying degree of relative importance to suit varying need and desires. A concurrent engineering team of experts from arena of heat exchanger and nanofluid to design required system possessing respective x-abilities, i.e. performance, maintenance,

heat transfer enhancement and modelisation of heat exchanger with nanofluid represented by four parallel paths in Figure 1 and lead the team to the final step of ranking and selection using TOPSIS method – a MADM approach.

Design goals. Design objectives are constructed to define the purpose of heat exchanger with required benchmark of performance and efficiency. Application that can be considered are whose performance abilities are already known. Some of common abilities that almost all heat exchanger possess with varying degree of importance based on its application.

Performance. Performance of heat exchanger plays a vital role in designing heat transfer with working fluid as nanofluid. It discusses the capability of the heat exchanger to consider all the parameters, constraints, accuracy and various techniques to enhance the performance. In this design goal, key design elements are topology in which heat exchanger have to perform, physical aspects of heat exchanger, control parameters considered in the application performance, material and accuracy.

Maintenance. Maintenance is a process of stabilising a condition or the state of being well-maintained in proper operational condition. Key attributes considered while designing heat exchanger for optimum maintenance are thermal aspects, constraints, challenges and performance. Maintenance is a key ability considered while designing of heat exchanger with nanofluid.

Heat transfer enhancement. Heat transfer performance enhancement plays a vibrant character in designing heat exchanger with nanofluid. Key design elements of this objective are surface area, density, thermal conductivity, specific heat capacity and constraints of effective thermophysical properties. The key objective of design flow is to meet this ability with high perfection concurrently considering all the other objectives. Hence, heat transfer enhancement is key design ability to be considered initially while designing heat exchanger with nanofluid.

Modelisation. Modelisation is a practice to design required heat exchanger with nanofluid considering all the thermal aspects, mechanical aspects, system aspects, application and measurement. Main challenge associated with modelisation of heat exchanger is working with nano-sized particles dispersed in heat transfer fluid to minimise the problem of sedimentation, agglomeration, pump loss, lack of stability, abrasion losses and additional flow resistance which may be in result to form scale in the path of flow in heat exchanger. So, modelisation is one of the key ability to be considered initially while designing heat exchanger working with nanofluid.

Design consideration for x-abilities of heat exchanger with nanofluid. After establishing design goals, succeeding step is to categorise all relevant attributes for each x-ability individually. Separate teams are formed for each x-ability that will work concurrently to reduce design cycle time. All design teams working on each abilities have to collect all the design information. For example, design team working on heat transfer enhancement ability is required to consider attributes like density, particle volume fraction, shape factor and nanolayer for thermal conductivity and specific heat capacity of nanofluid. Similarly, design team working on maintenance ability is required to consider attributes like sedimentation time, stability and pump loss for challenges that may be faced while working with nanofluid. In the next stage, various technological issues related to thermal aspects, mechanism constraints and control parameters and infrastructure issues related to physical aspects, environmental constraints, reliability and compactness are taken to be in description. This stage also include description of future requirements, research and development and how to obsolete challenges from designed system.

Identification of pertinent attributes for x-abilities. After categorising all relevant attributes for every x-ability, pertinent attributes for concurrent design of heat exchanger with nanofluid are identified from the broadly described array of x-abilities, i.e. performance, maintenance, heat transfer enhancement and modelisation. Following are some of the key attributes, which can be considered while designing heat exchanger with nanofluid:

- (1) Performance: topology, physical aspects, control parameters, material and accuracy.
- (2) Maintenance: thermal aspects, constraints, challenges and performance.
- (3) Heat transfer enhancement: surface area, density of nanofluid, thermal conductivity of nanofluid, heat capacity of nanofluid and constraints.
- (4) Modelisation: thermal aspects, mechanical aspects, system aspects, application aspect and measurement.

Identification and selection of attributes-based specifications of elements of heat exchanger with nanofluid. After selecting pertinent attributes, design team aim to identify and assign relative importance to elements of heat exchanger with nanofluid: nanoparticle, base fluid, channel, shape factor, maintenance required and so on, that are essential to attain the design goal. Specification of each identified element is considered one at a time for each of the pertinent attribute affecting x-abilities. These specification may possess qualitative or quantitative value and relative importance to each pertinent attribute is assigned via assigning values to relevant identified pertinent attribute. Relative importance is assigned to each specification based on number of relevant attributes that influence all x-abilities taken together. The identification of specification and relative importance of specifications of heat exchanger with nanofluid is achieved using fishbone diagram as shown in Figures 2-5. Fishbone diagram for each x-ability is prepared. Figures 2-5 represents fishbone diagram for performance, maintenance, heat transfer enhancement and modelisation of heat exchanger with nanofluid.

Fishbone diagram, i.e. cause and effect diagram is designed by systematically studying a problem or effect and to identify its causes in a design that resembles with the shape of fish. Figure 2 represents the fishbone diagram for performance of heat exchanger with nanofluid. All the attributes that add value to performance of heat exchanger with nanofluid are represented by major bones of fishbone diagram. For better performance of heat exchanger it require higher value of thermal conductivity, lower value of density, higher value of specific heat capacity. Similarly, performance of the designed system is based on the topology's subdivision factor, accuracy of designed system, physical infrastructure aspects and on the control parameters. For thorough study of performance of heat exchanger with nanofluid, attributes like material, topology, physical aspects, control parameters and accuracy that add value to performance are represented by major bone and its subdivision factors or subordinates like fluid flow, heat supplied, channel, system, working environment, sensitivity and so on are represented by sub-bones of the fishbone diagram. In this way, relevant specifications for the entire performance elements are identified and systematically represented in fishbone diagram in Figure 2.

Similarly, Figure 3 represents fishbone diagram for Maintenance of heat exchanger with nanofluid. All the attributes, like thermal aspects, constraints, challenges and performance that add value to maintenance of heat exchanger with nanofluid are represented by major bones in Figure 3. Thus in order to control the system

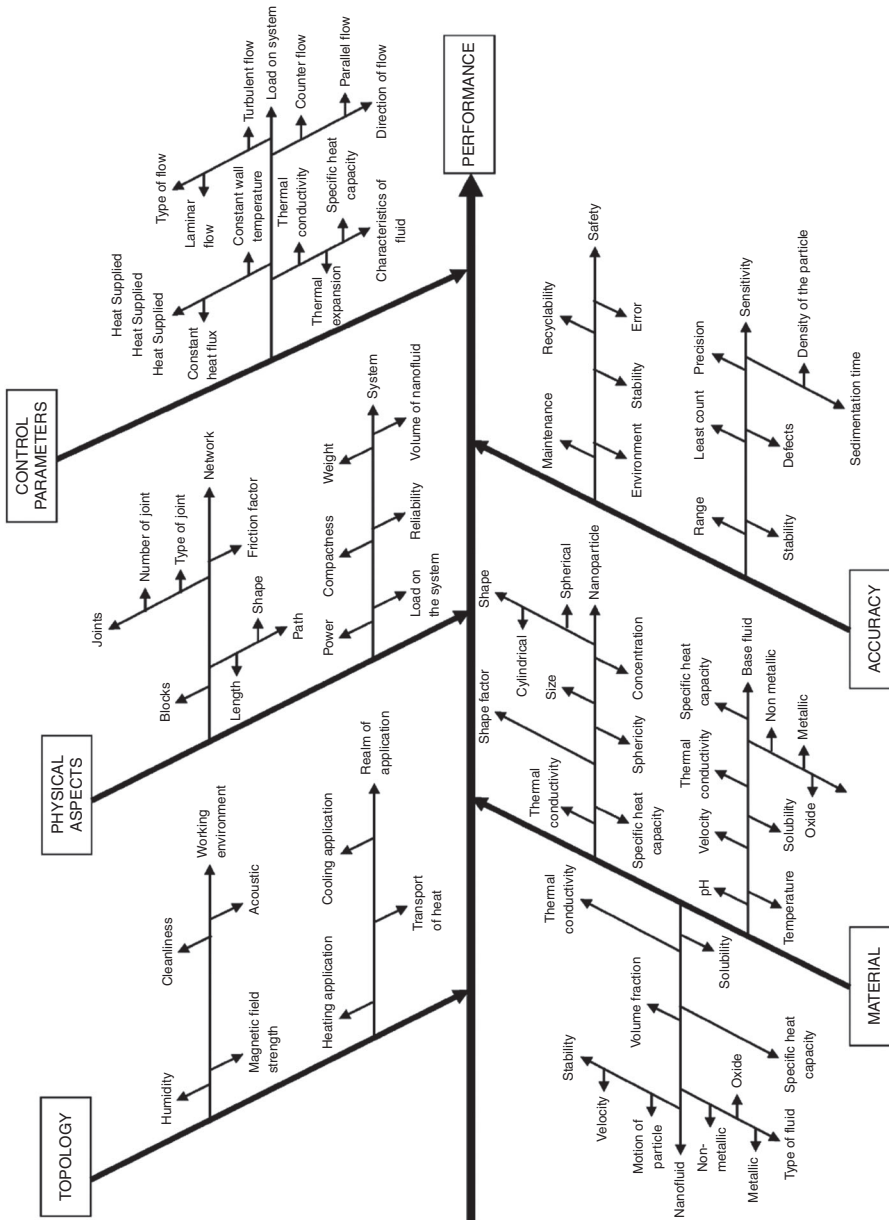


Figure 2. Fishbone diagram for performance of heat exchanger with nanofluid

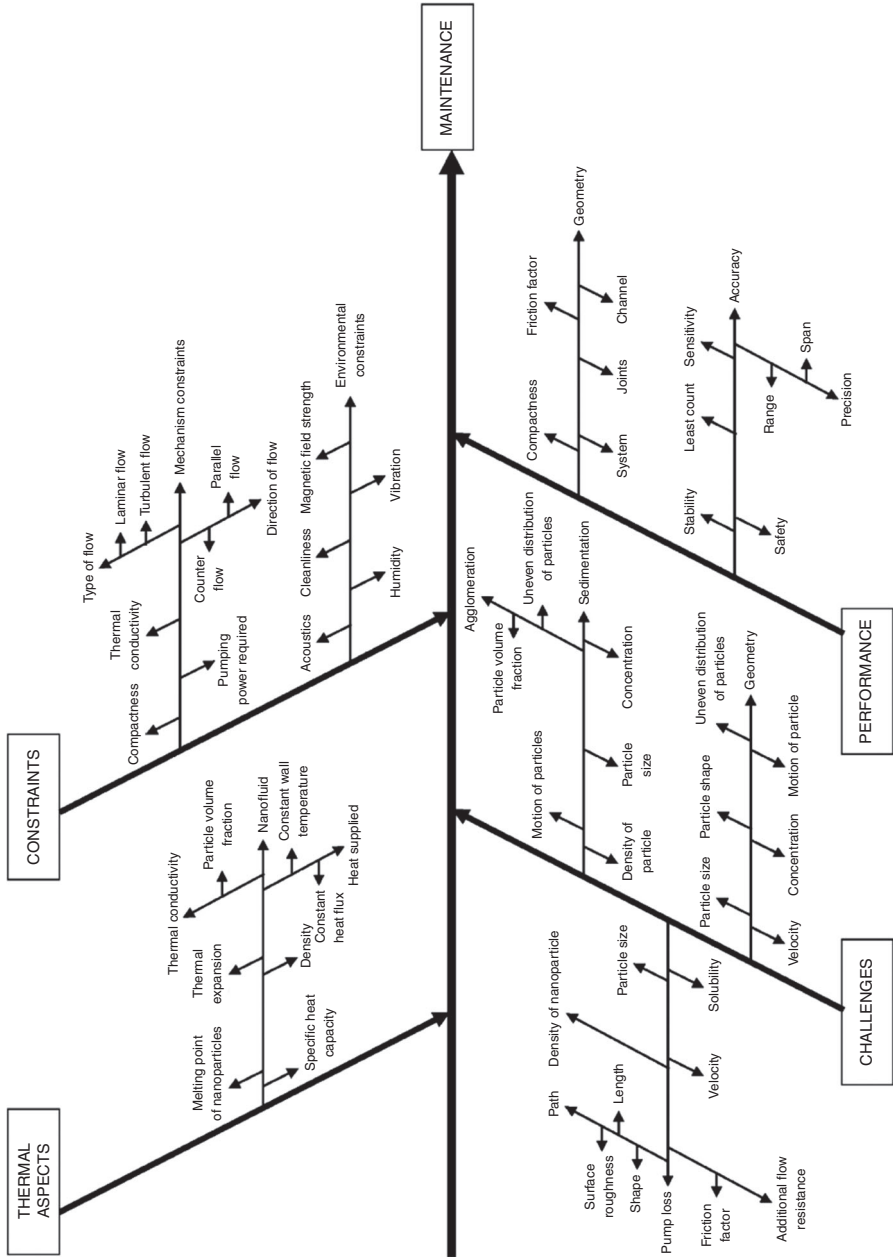


Figure 3. Fishbone diagram for maintenance of heat exchanger with nanofluid

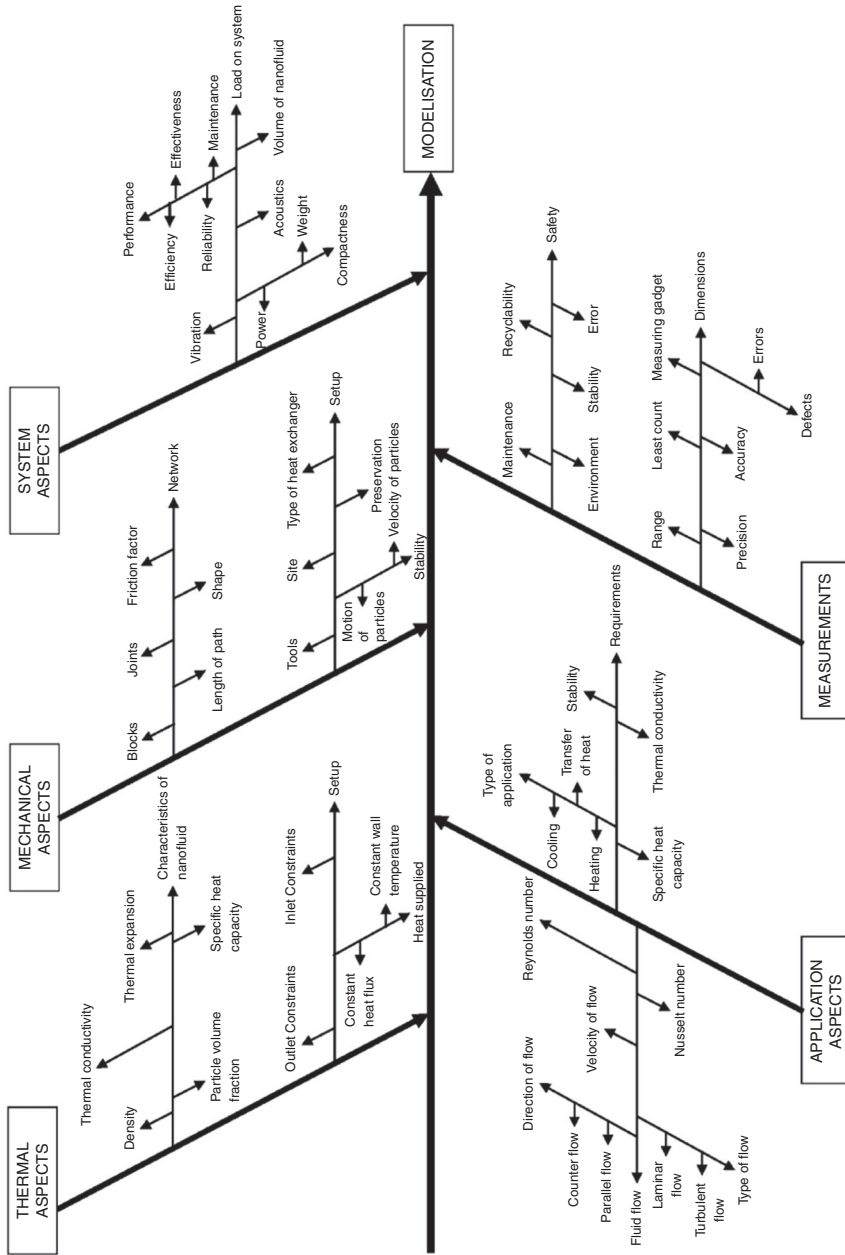


Figure 5.
Fishbone diagram
for modelisation
of heat exchanger
with nanofluid

displacement for better maintenance, better values of designed system elements are preferred. Better maintenance of heat exchanger with nanofluid depends on specifications of challenges faced in the designed system like, stability, pump loss, sedimentation, agglomeration and so on are represented by sub-bones. Likewise on the major bone of thermal aspects, thermophysical specifications of nanofluid like thermal conductivity, volume fraction, specific heat capacity, etc. and exhaustive specifications of heat supplied are represented on sub-bones. Similarly going for constraints and performance will result in thorough study of maintenance of heat exchanger with nanofluid and identifying and representing all the attributes accordingly will result in fishbone diagram of maintenance of heat exchanger with nanofluid in Figure 3.

Similarly, Figure 4 represents fishbone diagram for heat transfer enhancement of heat exchanger with nanofluid. All the attributes like surface area, thermal conductivity, density, heat capacity and constraints that add value to the key x-ability heat transfer enhancement are represented on the major bones. Thus in order to control thermal conductivity of the heat transfer fluid better specification of nanoparticle and base fluid are preferred, which give rise to improved heat transfer enhancement. On the major bone of thermal conductivity, specifications of nanoparticle and base fluid are represented by sub-bones. Specification of nanoparticles: thermal conductivity of nanoparticle, particle volume fraction, shape factor, sphericity and so on and specifications of base fluid: dipolarisation factor, dielectric constant, nanolayer, thermal conductivity are represented by sub-sub-bones. Similarly, after detailed examination to identify and systematically represent all the attributes on sub-bones that are responsible to form major bones like surface area, density and specific heat capacity for improved x-ability of heat transfer enhancement of heat exchanger with nanofluid will result in detailed fishbone diagram for the next x-ability, i.e. heat transfer enhancement in Figure 4.

Figure 5 represents fishbone diagram for modelisation of heat exchanger with nanofluid. All the attributes like thermal aspects, mechanical aspects, system aspects, application aspect and measurement that add value to the x-ability of modelisation of heat exchanger with nanofluid are represented on major bones. Thus in order to control elements of major bone influencing mechanical aspects of modelisation better specifications of network of channel and improved setup is required which will ultimately result to improved modelisation of the designed system. On the major bone of mechanical aspect elements influencing specifications of elements affecting network and setup are represented by sub-bones. Specification of network: blocks in network, nature of joints, friction factor, length of path of network, shape of network and elements affecting specification of the setup: tools used, site of the setup, type of heat exchanger used and control parameters of stability, i.e. motion of the particle and velocity of the particle are represented by further divided sub-bones. Similarly, after detailed examination to identify and systematically represent all the attributes by further dividing branches of bones that are responsible to form major bones like thermal aspect, mechanical aspect, system aspect, application aspect and measurements for improving x-ability modelisation of heat exchanger with nanofluid will ultimately results a thorough fishbone diagram for the modelisation of heat exchanger with nanofluid in Figure 5.

The entire process responsible for the design of Figures 2-5, i.e. identification, selection and representation of attribute-based specification of elements of nanofluid used are done concurrently by different teams for each x-ability to save time of the design process.

Assigning relative importance to these specifications. While considering all the mandatory pertinent attribute to design heat exchanger with best nanofluid available, the main requirement is to allot relative importance to every identified pertinent attributes according to needs and desires. For every process working under certain design constraints have different level of importance of each attribute over other attribute. Experts and specialists from different field allot relative importance to the specifications of pertinent attributes in relative to other pertinent attribute using different standards. One of the measure includes assigning values by identifying number of relevant features influence specification of x-abilities in fishbone diagram. For example, in the fishbone diagram of performance, maintenance, heat transfer enhancement and modelisation in Figures 2-5, it can be observed for pertinent attributes density, thermal conductivity, specific heat capacity and thermal expansion. Density influence 3, 4, 3, 2 relevant features, thermal conductivity influence 5, 6, 5, 4 relevant features, specific heat capacity influence 4, 5, 4, 3 relevant features and thermal expansion of nanofluid influence 2, 3, 2, 1 relevant features from all the four fishbone diagram, respectively. Taking on an average of number of times pertinent attributes influence relevant features of all x-abilities considering concurrently it is noted that density influence 3 relevant features, thermal conductivity influence 5 relevant features, specific heat capacity influence 4 relevant features and thermal expansion of nanofluid influence 2 relevant features. Further on the basis of this information relative importance quantitative values are assigned to every pertinent attribute accordingly. Higher the relative importance value attained by any attribute, more importance should be given to that attribute than other pertinent attributes. Relative importance values for improved x-abilities are assigned for every pertinent attributes as 1 for thermal expansion, 2 for density, 3 for specific heat capacity and 4 for thermal conductivity of nanofluid and represented in the mathematical form of relative importance matrix A . In A matrix, $i=j=1$ represent density, $i=j=2$ represent specific heat capacity, $i=j=3$ represent thermal conductivity, $i=j=4$ represent thermal expansion. $a_{i,j}$ represent relative importance of i over j . Therefore:

$$\begin{array}{cccc}
 a_{1, 1} = 2/2, & a_{1, 2} = 2/3, & a_{1, 3} = 2/4, & a_{1, 4} = 2/1 \\
 a_{2, 1} = 3/2, & a_{2, 2} = 3/3, & a_{2, 3} = 3/4, & a_{2, 4} = 3/1 \\
 a_{3, 1} = 4/2, & a_{3, 2} = 4/3, & a_{3, 3} = 4/4, & a_{3, 4} = 4/1 \\
 a_{4, 1} = 1/2, & a_{4, 2} = 1/3, & a_{4, 3} = 1/4, & a_{4, 4} = 1/1
 \end{array}$$

This method permits pairwise comparison of attributes only for a given application. Systematic and detailed examination of each x-ability is required to assign values of relative importance. Allotted values of relative importance to the pertinent attributes fluctuate from user to user with varying needs.

Ranking and selection using MADM three step approach. Systematic sequence of steps involved for the coding, evaluation, comparison, ranking and optimum selection of nanofluid for a heat exchanger are illustrated in Table I. Final selection of optimum nanofluid from the list of available nanofluids for any heat exchanger is done by MADM approach. All the feasible alternates of nanofluids satisfying the upper and lower bound of the attributes are considered. MADM approach applied over selected alternates of nanofluid in Table III to obtain goodness index of every

Stage 1: elimination stage

Scan the database for available nanofluids that satisfy the minimum requirement of all the pertinent attributes

Stage 2: evaluation step

$i = 1, 2, 3 \dots m$

$j = 1, 2, 3 \dots n$ where, m represents number of attributes-based specification of alternatives in rows and n represents number of attributes selected for characterisation of alternatives or pertinent attributes in columns

1. Decision matrix, D : identify specifications of corresponding pertinent attributes and represent it in the form of matrix:

$$D = [d_{ij}]_{m \times n}$$

d_{ij} represents elements of decision matrix

2. Normalised matrix, N : to bring magnitude of all pertinent attributes under the same range of 0-1 attribute/columnwise normalisation is done:

$$N = \left[\frac{d_{ij}}{\left(\sum_{i=1}^m d_{ij}^2 \right)^{\frac{1}{2}}} \right]_{m \times n}$$

3. Relative importance matrix, A :

$$A = \begin{bmatrix} \text{importance of } i\text{th attribute} \\ \text{importance of } j\text{th attribute} \end{bmatrix}_{n \times n}$$

4. Weight matrix, $W_{1 \times n}$:

$$(A - \lambda_{max} I) W^T = 0$$

weight matrix is to be customise in a form such that cumulative sum of all magnitudes of attributes is unity:

$$\sum_1 w_i = 1 \text{ and } W = [w_1, w_2, \dots, w_i, \dots, w_n]$$

5. Weighted normalised matrix, $Q = [q_{ij}]_{m \times n}$:

$$[q_{ij}]_{m \times n} = [n_{ij}]_{m \times n} \times [w_{ij}]_{1 \times n}$$

6. Positive ideal solution, S^+ and negative ideal solution, S^- :

$$S^+ = \{q_1^+, q_2^+, q_3^+, \dots, q_n^+\} = \{(\max q_{ij} | jL), (\min q_{ij} | jS)\}$$

$$S^- = \{q_1^-, q_2^-, q_3^-, \dots, q_n^-\} = \{(\min q_{ij} | jL), (\max q_{ij} | jS)\}$$

L is used for the benefit attributes that are larger the best for better heat transfer performance

S is used for the cost attributes that are smaller the best for better heat transfer performance

7. Separation measures Euclidean distance of selected nanofluid from the positive ideal solution in n -dimensional attribute space, D_i^+ :

$$D_i^+ = \left[\sum_{j=1}^n (q_{ij} - q_j^+)^2 \right]^{\frac{1}{2}}$$

Euclidean distance of selected nanofluid from the negative ideal solution in n -dimensional attribute space, D_i^- :

$$D_i^- = \left[\sum_{j=1}^n (q_{ij} - q_j^-)^2 \right]^{\frac{1}{2}}$$

8. Goodness Index, C_i^* : The relative closeness of feasible solution with respect to the positive ideal solution:

$$C_i^* = \frac{D_i^-}{D_i^+ + D_i^-}$$

$$0 \leq C_i^* \leq 1$$

Stage 3: ranking and selecting stage

Alternates are placed in increasing order of value of C_i^* .

Alternate with largest C_i^* is closest to D^+ and farthest from D^- .

The alternate having largest of C_i^* is preferred

Table I. MADM approach for ranking and selection of nanofluid

selected alternate. Available alternates are ordered on the basis of value of goodness index, C_i^* . Ranking of nanofluid for designed heat exchanger in order of preference is obtained by arranging C_i^* in decreasing order in Table II. The alternate having largest of C_i^* is preferred. This method ensures that the largest C_i^* candidate is closest to hypothetically best solution.

Procedure

Systematic sequence of steps involved in the procedure for the selection of best nanofluid in heat exchanger is presented in Figure 6 and all these steps are illustrated by an example presented in Table III:

- (1) Prepare cause and effect diagram for identification and selection of attributes-based specifications of heat exchanger with nanofluid as in Figures 2-5. Filter the attributes responsible for the causes identified from cause and effect diagram.
- (2) Collect the database of all the alternates of available nanofluid and filter out a list of eligible nanofluids that can be potentially applied in the required heat exchanger.
- (3) Collect the comprehensive and exhaustive information about the each attribute and selected alternates for the precise quantitative and qualitative coding of each attributes for every selected alternatives that is beneficial for evaluation and selection procedure. To simplify classification and differentiation of different nanofluids based on the identified attributes, coding scheme is developed.
- (4) Filter out few pertinent attributes which will directly affect the performance of nanofluid in heat exchanger that are sufficient for the selection procedure. Upper and lower limits of values for these pertinent attributes is allotted by exhaustive information from a team of users and experts for a particular application. Therefore, further the procedure move with selected list of attributes eliminating the rest.
- (5) Develop decision matrix in terms of attributes for accepted alternates of nanofluid in which alternates are defined by rows and pertinent attributes are defined by columns. Normalising of decision matrix is done to bring magnitude of pertinent attributes of all the selected alternates under the same range of 0-1.
- (6) Assign relative importance matrix. Weight vectors are calculated from the relative importance matrix to moderate the error in inconsistency of relative importance values.
- (7) Finally a weighted normalise matrix is developed from the weight vector matrix and normalised matrix for the selected alternates of nanofluid.
- (8) Selected optimum nanofluid must be closest to the positive ideal solution and farthest away from the negative ideal solution. So, hypothetically best and worst solutions are assumed from the weighted normalised matrix.
- (9) Calculate Euclidean distance of all the nanofluids from the assumed positive and negative ideal solution.
- (10) Relative closeness or suitability index or goodness index means the relative closeness of all the nanofluids with respect to the hypothetical ideal nanofluid. Ranking is done the increasing order of magnitude of suitability index for every alternate. Higher the value of suitability index better is the alternate.
- (11) The alternate having largest of suitability index is selected.

Sensitivity analysis

Available nanoparticles are Al_2O_3 , Cu, CuO, SiO_2 and TiO_2 with water as a base fluid.

It can be observed from the above calculated data in Figure 7 that, density of all the considered alternate of nanofluid goes on increasing with increasing particle volume fraction. For example, in Figure 7 considering Al_2O_3 (nanoparticle) + base fluid (water), for pure base fluid (i.e. 0 per cent of particle volume fraction of Al_2O_3 nanoparticle), density observed is 997.1. With the addition of 5 per cent of Al_2O_3 nanoparticle in base fluid to make nanofluid of density 1,145.745, i.e. 14.91 per cent increased density of the designed nanofluid as compared to base fluid is observed. Same observation was

Alternates	C_i^*	5% Ranking	C_i^*	10% Ranking	C_i^*	15% Ranking	C_i^*	20% Ranking
Al_2O_3	0.3691	4th	0.3895	4th	0.4083	4th	0.4254	4th
Cu	0.9997	1st	0.9996	1st	0.9996	1st	0.9995	1st
CuO	0.6493	2nd	0.6545	2nd	0.6595	2nd	0.6641	2nd
SiO_2	0.0019	5th	0.0024	5th	0.0028	5th	0.0034	5th
TiO_2	0.3806	3rd	0.3973	3rd	0.4125	3rd	0.4263	3rd

Table II.
Ranking of nanofluid

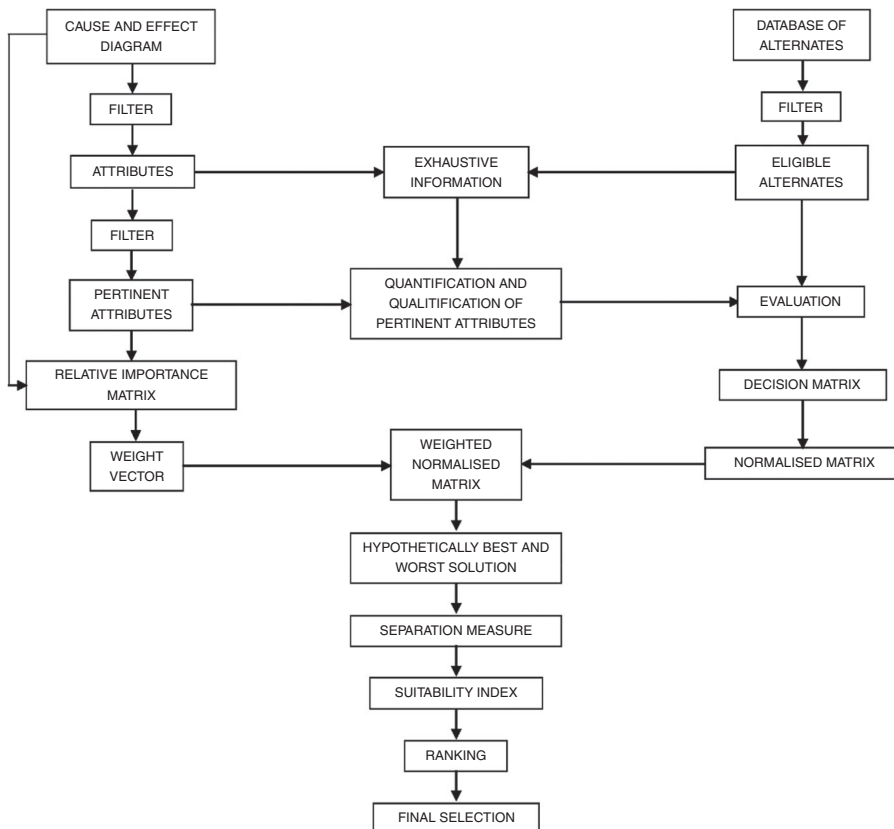


Figure 6.
Flow chart of step
by step procedure
for selection by
CE-MADM approach

Table III.
Illustrative examples
on MADM approach

$\phi = 5\%$	$\phi = 10\%$	$\phi = 15\%$	$\phi = 20\%$
Decision matrix, D $\begin{bmatrix} 1.145,745 & 2,7874 \times 10^{-4} & 0,7027 & 5,001,876 \\ 1,394,945 & 3,3776 \times 10^{-4} & 0,7093 & 5,010,447 \\ 1,272,245 & 3,0775 \times 10^{-4} & 0,7001 & 5,001,876 \\ 1,060,745 & 2,6050 \times 10^{-4} & 0,6410 & 5,011,903 \\ 1,159,745 & 2,8221 \times 10^{-4} & 0,6967 & 5,011,376 \end{bmatrix}$	Decision matrix, D $\begin{bmatrix} 1,294,39 & 3,1929 \times 10^{-4} & 0,8015 & 5,267,316 \\ 1,792,79 & 4,3800 \times 10^{-4} & 0,8163 & 5,286,334 \\ 1,547,39 & 3,7730 \times 10^{-4} & 0,7958 & 5,267,316 \\ 1,124,39 & 2,8271 \times 10^{-4} & 0,6698 & 5,289,606 \\ 1,322,39 & 3,2634 \times 10^{-4} & 0,78839 & 5,288,431 \end{bmatrix}$	Decision matrix, D $\begin{bmatrix} 1,443,035 & 3,6099 \times 10^{-4} & 0,9111 & 5,562,508 \\ 2,190,635 & 5,4006 \times 10^{-4} & 0,9358 & 5,594,405 \\ 1,822,535 & 4,4798 \times 10^{-4} & 0,9016 & 5,562,509 \\ 1,188,035 & 3,0601 \times 10^{-4} & 0,6996 & 5,599,891 \\ 1,485,035 & 3,7174 \times 10^{-4} & 0,8893 & 5,597,916 \end{bmatrix}$	Decision matrix, D $\begin{bmatrix} 1,591,68 & 4,0389 \times 10^{-4} & 1,033 & 5,692,752 \\ 2,588,48 & 6,4400 \times 10^{-4} & 1,070 & 5,940,570 \\ 2,097,68 & 5,1981 \times 10^{-4} & 1,019 & 5,692,752 \\ 1,251,68 & 3,3048 \times 10^{-4} & 0,7302 & 5,948,840 \\ 1,647,68 & 4,1846 \times 10^{-4} & 1,0007 & 5,945,869 \end{bmatrix}$
Normalised matrix, N $\begin{bmatrix} 0,4227 & 0,4231 & 0,4552 & 0,4467 \\ 0,5146 & 0,5127 & 0,4595 & 0,4475 \\ 0,4694 & 0,4672 & 0,4535 & 0,4467 \\ 0,3913 & 0,3954 & 0,4152 & 0,4476 \\ 0,4279 & 0,4284 & 0,4513 & 0,4476 \end{bmatrix}$	Normalised matrix, N $\begin{bmatrix} 0,4034 & 0,4047 & 0,4618 & 0,4461 \\ 0,5587 & 0,5551 & 0,4703 & 0,4478 \\ N = \begin{bmatrix} 0,4822 & 0,4782 & 0,4585 & 0,4461 \\ 0,3503 & 0,3583 & 0,3859 & 0,4480 \\ 0,4121 & 0,4136 & 0,4542 & 0,4479 \end{bmatrix} \end{bmatrix}$	Normalised matrix, N $\begin{bmatrix} 0,3982 & 0,3905 & 0,4674 & 0,4455 \\ 0,5893 & 0,5842 & 0,4801 & 0,4481 \\ 0,4903 & 0,4846 & 0,4626 & 0,4485 \\ 0,3196 & 0,3310 & 0,3589 & 0,4485 \\ 0,3995 & 0,4021 & 0,4562 & 0,4484 \end{bmatrix}$	Normalised matrix, N $\begin{bmatrix} 0,3760 & 0,3795 & 0,4722 & 0,4448 \\ 0,6115 & 0,6032 & 0,4891 & 0,4484 \\ 0,4956 & 0,4885 & 0,4658 & 0,4448 \\ 0,2957 & 0,3105 & 0,3538 & 0,4491 \\ 0,3893 & 0,3932 & 0,4575 & 0,4488 \end{bmatrix}$
Relative importance matrix, A $\begin{bmatrix} 2/2 & 2/3 & 2/4 & 2/1 \\ 3/2 & 3/3 & 3/4 & 3/1 \\ 4/2 & 4/3 & 4/4 & 4/1 \\ 1/2 & 1/3 & 1/4 & 1/1 \end{bmatrix}$	Relative importance matrix, A $\begin{bmatrix} 2/2 & 2/3 & 2/4 & 2/1 \\ 3/2 & 3/3 & 3/4 & 3/1 \\ 4/2 & 4/3 & 4/4 & 4/1 \\ 1/2 & 1/3 & 1/4 & 1/1 \end{bmatrix}$	Relative importance matrix, A $\begin{bmatrix} 2/2 & 2/3 & 2/4 & 2/1 \\ 3/2 & 3/3 & 3/4 & 3/1 \\ 4/2 & 4/3 & 4/4 & 4/1 \\ 1/2 & 1/3 & 1/4 & 1/1 \end{bmatrix}$	Relative importance matrix, A $\begin{bmatrix} 2/2 & 2/3 & 2/4 & 2/1 \\ 3/2 & 3/3 & 3/4 & 3/1 \\ 4/2 & 4/3 & 4/4 & 4/1 \\ 1/2 & 1/3 & 1/4 & 1/1 \end{bmatrix}$
Relative weight vector $\begin{bmatrix} w_1 \\ w_2 \\ w_3 \\ w_4 \end{bmatrix} = \begin{bmatrix} 0,2 \\ 0,3 \\ 0,4 \\ 0,1 \end{bmatrix}$	Relative weight vector $\begin{bmatrix} w_1 \\ w_2 \\ w_3 \\ w_4 \end{bmatrix} = \begin{bmatrix} 0,2 \\ 0,3 \\ 0,4 \\ 0,1 \end{bmatrix}$	Relative weight vector $\begin{bmatrix} w_1 \\ w_2 \\ w_3 \\ w_4 \end{bmatrix} = \begin{bmatrix} 0,2 \\ 0,3 \\ 0,4 \\ 0,1 \end{bmatrix}$	Relative weight vector $\begin{bmatrix} w_1 \\ w_2 \\ w_3 \\ w_4 \end{bmatrix} = \begin{bmatrix} 0,2 \\ 0,3 \\ 0,4 \\ 0,1 \end{bmatrix}$
Weighted normalised matrix, \bar{Q} $\begin{bmatrix} 0,0845 & 0,1269 & 0,1821 & 0,0447 \\ 0,1029 & 0,1538 & 0,1838 & 0,0447 \\ 0,0939 & 0,1401 & 0,1814 & 0,0447 \\ 0,0783 & 0,1186 & 0,1661 & 0,0448 \\ 0,0856 & 0,1285 & 0,1805 & 0,0448 \end{bmatrix}$	Weighted normalised matrix, \bar{Q} $\begin{bmatrix} 0,0807 & 0,1214 & 0,1847 & 0,0446 \\ 0,1117 & 0,1665 & 0,1881 & 0,0448 \\ 0,0964 & 0,1434 & 0,1834 & 0,0448 \\ 0,0701 & 0,1075 & 0,1544 & 0,0448 \\ 0,0824 & 0,1241 & 0,1817 & 0,0448 \end{bmatrix}$	Weighted normalised matrix, \bar{Q} $\begin{bmatrix} 0,0776 & 0,1171 & 0,1870 & 0,0448 \\ 0,1076 & 0,1753 & 0,1920 & 0,0448 \\ 0,0980 & 0,1454 & 0,1850 & 0,0445 \\ 0,0639 & 0,0993 & 0,1436 & 0,0448 \\ 0,0799 & 0,1206 & 0,1825 & 0,0448 \end{bmatrix}$	Weighted normalised matrix, \bar{Q} $\begin{bmatrix} 0,0752 & 0,1139 & 0,1889 & 0,0445 \\ 0,1223 & 0,1815 & 0,1956 & 0,0448 \\ 0,0991 & 0,1465 & 0,1863 & 0,0445 \\ 0,0591 & 0,0931 & 0,1335 & 0,0449 \\ 0,0778 & 0,1180 & 0,1830 & 0,0449 \end{bmatrix}$
Positive ideal and negative ideal solution $S^+ = (0,1029, 0,1538, 0,1838, 0,0448)$ $S^- = (0,0783, 0,1186, 0,1664, 0,0447)$	Positive ideal and negative ideal solution $S^+ = (0,1117, 0,1665, 0,1881, 0,0448)$ $S^- = (0,0701, 0,1075, 0,1544, 0,0446)$	Positive ideal and negative ideal solution $S^+ = (0,1178, 0,1753, 0,1920, 0,0448)$ $S^- = (0,0639, 0,0993, 0,1436, 0,0445)$	Positive ideal and negative ideal solution $S^+ = (0,1223, 0,1815, 0,1956, 0,0449)$ $S^- = (0,0591, 0,0931, 0,1335, 0,0445)$
Separation measures from positive and negative ideal solution $P = (0,0326, 0,000013, 0,0165, 0,9464, 0,0308)$ $L = (0,0191, 0,0464, 0,0307, 0,000095, 0,0189)$	Separation measures from positive and negative ideal solution $P = (0,0549, 0,000027, 0,0281, 0,0797, 0,0520)$ $L = (0,0350, 0,0797, 0,0532, 0,0002, 0,0343)$	Separation measures from positive and negative ideal solution $P = (0,0708, 0,00004, 0,0365, 0,1050, 0,0672)$ $L = (0,0489, 0,1050, 0,0707, 0,0003, 0,0472)$	Separation measures from positive and negative ideal solution $P = (0,0827, 0,00006, 0,0430, 0,1251, 0,0786)$ $L = (0,0612, 0,1251, 0,0850, 0,0004, 0,0584)$
Relative closeness to positive benchmark index $C = (0,3691, 0,9997, 0,6493, 0,0019, 0,3806)$	Relative closeness to positive benchmark index $C = (0,3895, 0,9996, 0,6545, 0,0024, 0,3973)$	Relative closeness to positive benchmark index $C = (0,4083, 0,9996, 0,6595, 0,0028, 0,4125)$	Relative closeness to positive benchmark index $C = (0,4254, 0,9995, 0,6641, 0,0034, 0,4263)$

performed and analysed with the addition of 10, 15 and 20 per cent of Al_2O_3 nanoparticle in water. With the addition of 10 per cent of Al_2O_3 nanoparticle in water there will be 12.97 per cent increase in value of density as compared to nanofluid with 5 per cent particle volume fraction, and the value of density enhances to 1,294.39. On further continuing the observation for 15 and 20 per cent, similar results were found. With 15 per cent particle volume fraction of Al_2O_3 value of density enhanced to 1,443.035, i.e. 11.48 per cent increase in density as compared to 10 per cent particle volume fraction of Al_2O_3 was observed. And with the addition of 20 per cent particle volume fraction of Al_2O_3 value of density will increased to 1,591.68, i.e. 10.30 per cent increase in density as compared to 15 per cent particle volume fraction of Al_2O_3 was observed and percentage increase in density was represented in Figure 11(a). The point to be get noticed in Figure 11(a) is that rather the density is increasing with increasing particle volume fraction, but height of percentage increase of density get relatively lowered at every step of increasing particle volume fraction, i.e. height of percentage increase of density for 5, 10, 15 and 20 per cent gets relatively lowered for every step from 14.91 to 12.97 per cent to 11.48 to 10.30 per cent, respectively. Same experiment was performed for nanoparticles of Cu, CuO, SiO_2 and TiO_2 . In case of Cu, density for 0 per cent of particle volume fraction (i.e. pure base fluid) of copper nanoparticles in water is 997.1 and with addition of 5, 10, 15 and 20 per cent particle volume fraction of Cu nanoparticle in water, density got increased to 1,394.945, 1,792.79, 2,190.635 and 2,588.48, respectively represented in Figure 7. And height of percentage increase of density for 5, 10, 15, and 20 per cent gets comparatively depressed for each stage from 14.91 to 12.97 per cent to 11.48 to 10.30 per cent, respectively is represented in Figure 11(a). In case of CuO, density for 0 per cent of particle volume fraction (i.e. pure base fluid) of CuO nanoparticles in water is 997.1 and with addition of 5, 10, 15 and 20 per cent particle volume fraction of CuO nanoparticle in water, density got increased to 1,272.245, 1,547.39, 1,822.535 and 2,097.68, respectively is represented in Figure 7. And height of percentage increase of density for 5, 10, 15, and 20 per cent gets comparatively depressed for each stage from 27.59 to 21.62 per cent to 17.78 to 15.09 per cent, respectively is represented in Figure 11(a). In case of SiO_2 , density for 0 per cent of particle volume fraction (pure base fluid) of SiO_2 nanoparticles in water is 997.1 and with addition of 5, 10, 15 and 20 per cent particle volume fraction of SiO_2 nanoparticle in water density got increased to 1,060.745, 1,124.39, 1,188.035 and 1,251.68, respectively is represented in Figure 7. And height of percentage increase of density for 5, 10, 15 and 20 per cent gets comparatively depressed for each stage from 6.38 to 6.00 to 5.66 to 5.36 per cent, respectively is represented in Figure 11(a). In case of TiO_2 , density for 0 per cent of particle volume fraction (pure base fluid) of TiO_2 nanoparticles in water is 997.1 and with addition of 5, 10, 15 and 20 per cent particle volume fraction of TiO_2 nanoparticle in water density got increased to 1,159.745, 1,322.39, 1,480.035 and 1,647.68, respectively is represented in Figure 7. And height of percentage increase of

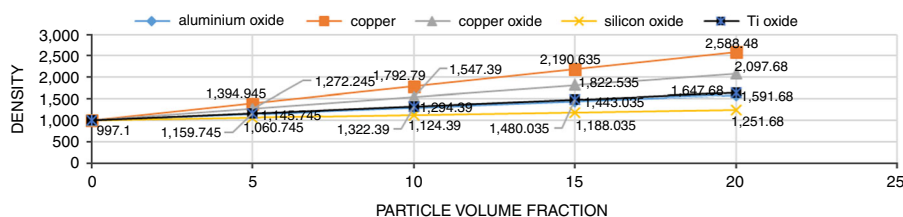


Figure 7.
Density of
nanofluids with
varying particle
volume fraction

density for 5, 10, 15 and 20 per cent gets comparatively depressed for each stage from 16.31 to 14.02 per cent to 11.92 to 11.33 per cent, respectively is represented in Figure 11(a).

Studying the behaviour of heat capacity with varying particle volume fraction in Figure 8 for different considered nanofluids, it is observed that heat capacity of nanofluid goes on constantly decreasing with increasing particle volume fraction. For example, observing behaviour of Al_2O_3 nanoparticle with water as base fluid in Figure 8, heat capacity of pure base fluid (0 per cent particle volume fraction of Al_2O_3 nanoparticle in water) is 4,179. With the addition of 5 per cent of Al_2O_3 nanoparticle in water to form a nanofluid, its heat capacity will get decreased to 3,587.525, i.e. 14.15 per cent of decrement in value of heat capacity was observed as compared to pure base fluid and percentage decrement in value of hate capacity is represented in Figure 11(b). Further observing the same experiment with the addition of 10 per cent particle volume fraction of Al_2O_3 nanoparticle in water, heat capacity will get further decreased by 12.70 per cent and new value of heat capacity of formed nanofluid will become 3,131.898. Performing the same experiment on nanofluid with particle volume fraction of 15 and 20 per cent Al_2O_3 nanoparticle in water, heat capacity of formed nanofluid will further reduced to 2,770.138 in 15 per cent to 2,475.946 in 20 per cent particle volume fraction, respectively, i.e. 11.55 and 10.62 per cent decrement was noted. The thing to be get observed is that as the heat capacity of Al_2O_3 nanofluid is decreased with increasing particle volume fraction, but height of percentage decreased of heat capacity get lowered at every step of increasing particle volume fraction as, the height of percentage decrease of heat capacity of Al_2O_3 nanofluid with 5, 10, 15 and 20 per cent particle volume fraction of Al_2O_3 nanoparticle in water gets relatively lowered for every step from 14.15 to 12.70 per cent to 11.55 to 10.62 per cent, respectively is represented in Figure 11(b). Similarly, repeating the same observation for varying particle volume fraction of Cu, CuO, SiO_2 and TiO_2 nanoparticles in Figure 8 and Figure 11(b). In case of Cu, heat capacity for 0 per cent of particle volume fraction, i.e. pure base fluid without any copper nanoparticles in water is 4,179 and with addition of 5, 10, 15 and 20 per cent particle volume fraction of Cu nanoparticle in water, heat capacity got decreased from 4,179 to 2,960.694 to 2,283.107 to 1,851.635 to 1,552.79, respectively in Figure 8. And in Figure 11(b), height of percentage decrease of heat capacity for 5, 10, 15 and 20 per cent gets comparatively depressed for each stage from 14.15 to 12.70 per cent to 11.55 to 10.62 per cent, respectively. In case of CuO, heat capacity for 0 per cent of particle volume fraction (i.e. pure base fluid) of CuO nanoparticles in water is 4,179 and with addition of 5, 10, 15 and 20 per cent particle volume fraction of CuO nanoparticle in water, heat capacity got depressed from 4,179 to 3,249.403 to 2,650.394 to 2,232.247 to 1,923.794, respectively in Figure 8. And in Figure 11(b), height of percentage decrement of heat capacity of CuO nanoparticles in water with particle volume fraction of 5, 10, 15 and 20 per cent gets comparatively depressed at each stage from 22.24 to 18.43 per cent to 15.77 to 13.82 per cent, respectively. In case of SiO_2 , heat capacity for 0 per cent of

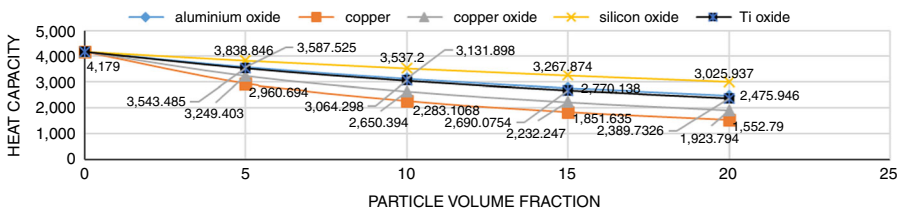


Figure 8.
Heat capacity of nanofluids with varying particle volume fraction

particle volume fraction of SiO_2 nanoparticles in water (i.e. pure base fluid) is 4,179 and with addition of 5, 10, 15 and 20 per cent particle volume fraction of SiO_2 nanoparticle in water in Figure 8, heat capacity got decreased to 3,838.846, 3,537.200, 3,267.874 and 3,025.937, respectively. And in Figure 11(b) height of percentage decrement of heat capacity for 5, 10, 15 and 20 per cent particle volume fraction of SiO_2 nanoparticle in water gets comparatively depressed for each stage from 8.14 to 7.86 per cent to 7.61 to 7.40 per cent, respectively. In case of TiO_2 , heat capacity for 0 per cent of particle volume fraction of TiO_2 nanoparticles in water (i.e. pure base fluid) is 4,179 and with addition of 5, 10, 15 and 20 per cent particle volume fraction of TiO_2 nanoparticle in water, heat capacity got decreased to 3,543.485, 3,064.298, 2,690.075 and 2,389.753, respectively as represented in Figure 8. And in Figure 11(b) height of percentage decrease of heat capacity of nanofluid for 5, 10, 15 and 20 per cent particle volume fraction of TiO_2 nanoparticles in water gets comparatively depressed on each stage from 15.21 to 13.52 per cent to 12.21 to 11.16 per cent, respectively.

Similarly, performing same experiment to measure height of variation of thermal conductivity and thermal expansion of various nanofluid with varying particle volume fraction is observed and represented as a graph in Figures 9 and 10. It was observed that thermal conductivity of nanofluid goes on constantly growing with increasing particle volume fraction represented in Figure 11(c) and thermal expansion of nanofluid goes on constantly decreasing with increasing particle volume fraction represented in Figure 11(d). Observing the behaviour of thermal conductivity of various nanofluid with varying particle volume fraction from Figure 9. Thermal conductivity of all the considered varieties nanofluids exhibits the property of increase in thermal conductivity with increasing particle volume fraction. For example, observing behaviour of Al_2O_3 nanoparticle in water as base fluid in Figure 9, thermal conductivity of pure base fluid (0 per cent particle volume fraction of Al_2O_3 nanoparticle in water) is 0.613. With the addition of 5 per cent of Al_2O_3 nanoparticle in water to form nanofluid, its thermal conductivity will increased to 0.7027, i.e. 14.63 per cent of increment in value of thermal conductivity was observed as compared to pure base fluid and percentage increase in value of thermal conductivity is represented in Figure 11(c). With further addition of nanoparticles of Al_2O_3 in water to the concentration of 10 per cent particle volume fraction, thermal conductivity will further increased by 14.06 per cent and new

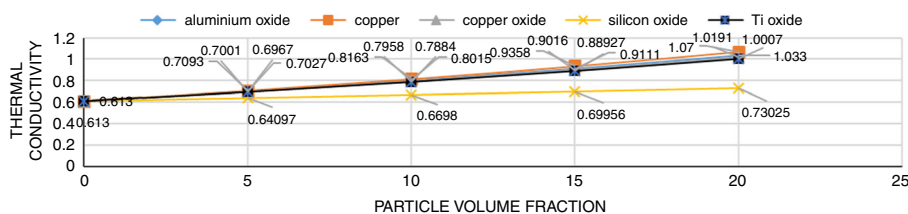


Figure 9.

Thermal conductivity of nanofluids with varying particle volume fraction

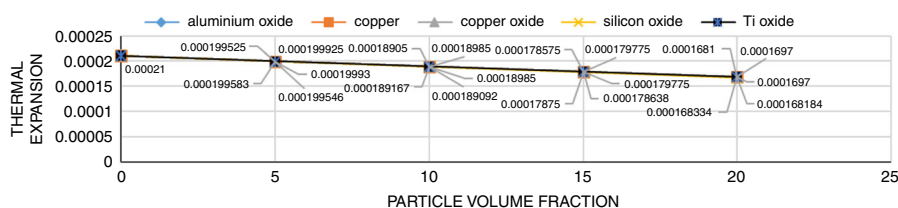


Figure 10.

Thermal expansion of nanofluids with varying particle volume fraction

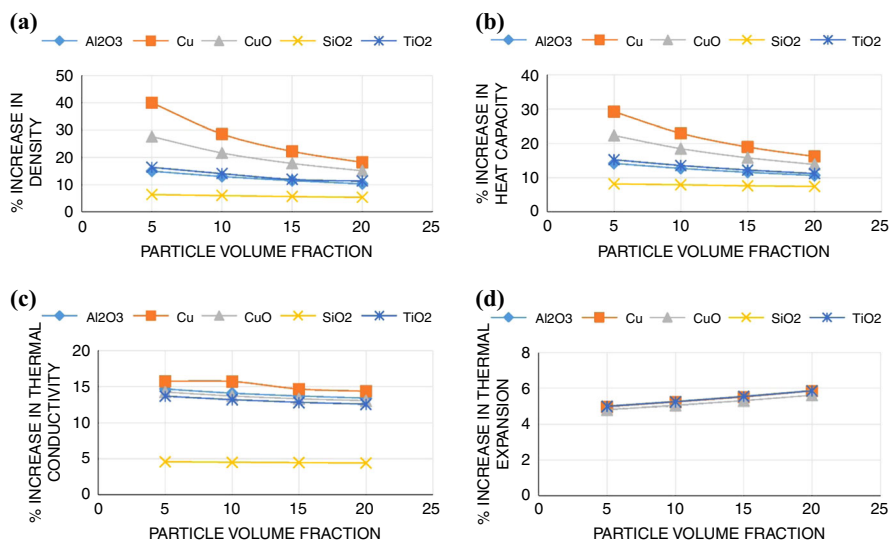


Figure 11. Percentage variation of pertinent attributes with varying particle volume fraction

Notes: (a) Percentage variation in density with varying particle volume fraction; (b) percentage variation in heat capacity with varying particle volume fraction; (c) percentage variation in thermal conductivity with varying particle volume fraction; (d) percentage variation in thermal expansion with varying particle volume fraction

observed value of thermal conductivity of formed nanofluid will become 0.8015. with further addition of Al₂O₃ nanoparticle in water to particle volume fraction from 10 to 15 to 20 per cent, thermal conductivity will further increased from 0.8015 to 0.9111 to 1.033, respectively, i.e. 13.67 per cent increment in 15 and 13.38 per cent increment in 20 per cent is noted. In Figure 11(c), it is clearly observed that thermal conductivity of Al₂O₃ nanofluid is increasing with increasing particle volume fraction, but height of percentage increase in thermal conductivity get reduced at every step of 5 per cent increase in particle volume fraction. Height of percentage increase of thermal conductivity of Al₂O₃ nanofluid with 5 to 10 to 15 to 20 per cent particle volume fraction of Al₂O₃ nanoparticle in water gets relatively lowered in every step from 14.63 to 14.06 to 13.67 to 13.38 per cent, respectively. Similarly, repeating the same observation for varying particle volume fraction of Cu, CuO, SiO₂ and TiO₂ nanoparticles to draw Figures 9 and 11(c). In case of Cu, thermal conductivity for 0 per cent of particle volume fraction, i.e. pure base fluid without any copper nanoparticles in water is 0.613 and with addition of 5, 10, 15 and 20 per cent particle volume fraction of Cu nanoparticle in water, thermal conductivity get increased from 0.613 to 0.7093 to 0.8163 to 0.9358 to 1.070, respectively in Figure 9. And in Figure 11(c), height of percentage increment in thermal conductivity for 5, 10, 15 and 20 per cent gets comparatively depressed in each stage from 15.71 to 15.08 to 14.64 to 14.34 per cent, respectively. In case of CuO, thermal conductivity for 0 per cent of particle volume fraction (i.e. pure base fluid) of CuO nanoparticles in water is 0.613 and with addition of 5, 10, 15 and 20 per cent particle volume fraction of CuO nanoparticle in water, thermal conductivity get increased from 0.613 to 0.7001 to 0.7958 to 0.9016 to 1.0191, respectively in Figure 9. And in Figure 11(c), height of percentage increment of thermal conductivity of CuO nanoparticles in water with particle volume fraction of 5, 10, 15 and 20 per cent gets comparatively depressed at each stage from 14.21 to 13.67 to 13.29 to

13.03 per cent, respectively. In case of SiO_2 , thermal conductivity for 0 per cent of particle volume fraction of SiO_2 nanoparticles in water (i.e. pure base fluid) is 0.613 and with addition of 5, 10, 15 and 20 per cent particle volume fraction of SiO_2 nanoparticle in water in Figure 9, thermal conductivity get increased to 0.64097 to 0.6698 to 0.69956 to 0.73025, respectively. And in Figure 11(c) height of percentage increment in thermal conductivity for 5, 10, 15, and 20 per cent particle volume fraction of SiO_2 nanoparticle in water gets comparatively depressed for each stage from 4.56 to 4.49 to 4.44 to 4.39 per cent, respectively. In case of TiO_2 , thermal conductivity for 0 per cent of particle volume fraction of TiO_2 nanoparticles in water (i.e. pure base fluid) is 0.613 and with addition of 5, 10, 15 and 20 per cent particle volume fraction of TiO_2 nanoparticle in water, thermal conductivity get increased to 0.6967, 0.78839, 0.88927 and 1.0007, respectively as represented in Figure 9. And in Figure 11(c) height of percentage increase of thermal conductivity of nanofluid for 5, 10, 15 and 20 per cent particle volume fraction of TiO_2 nanoparticles in water gets comparatively depressed on each stage from 13.65 to 13.16 to 12.79 to 12.53 per cent, respectively.

It can be observed from Figure 10 that, thermal expansion of all the considered alternate of nanofluid goes on decreasing with increasing particle volume fraction. For example, in Figure 10 considering Al_2O_3 (nanoparticle) + base fluid (water), for pure base fluid (i.e. 0 per cent of particle volume fraction of Al_2O_3 nanoparticle), thermal expansion observed is 21×10^{-5} . With the addition of 5 per cent of Al_2O_3 nanoparticle in base fluid to make nanofluid with thermal expansion of 19.99×10^{-5} , i.e. 4.81 per cent decreased thermal expansion of the designed nanofluid as compared to base fluid is observed. Same observation was performed and analysed with the addition of 10, 15 and 20 per cent of Al_2O_3 nanoparticle in water. With the addition of 10 per cent of Al_2O_3 nanoparticle in water there will be 5.03 per cent decrease in value of thermal expansion as compared to nanofluid with 5 per cent particle volume fraction, and the value of thermal expansion will reduced to 18.985×10^{-5} . On further continuing the observation for 15 and 20 per cent, similar results were found. With 15 per cent particle volume fraction of Al_2O_3 value of thermal expansion reduced to 17.9775×10^{-5} , i.e. 5.30 per cent decrease in thermal expansion as compared to 10 per cent particle volume fraction of Al_2O_3 was observed. And with the addition of 20 per cent particle volume fraction of Al_2O_3 value of thermal expansion will decreased to 16.97×10^{-5} , i.e. 5.60 per cent decrease in thermal expansion as compared to 15 per cent particle volume fraction of Al_2O_3 was observed and percentage decrement in thermal expansion was represented in Figure 11(d). The thing to be get noticed in Figure 11(d) is that rather the thermal expansion is decreased with increasing particle volume fraction, but height of percentage decrease of thermal expansion get relatively increased at every step of increasing particle volume fraction, i.e. height of percentage decrease of thermal expansion for 5, 10, 15 and 20 per cent gets relatively increased for every step from 4.81 to 5.03 to 5.30 to 5.60 per cent, respectively. Same experiment was performed for nanoparticles of Cu, CuO, SiO_2 and TiO_2 . In case of Cu, thermal expansion for 0 per cent of particle volume fraction (i.e. pure base fluid) of copper nanoparticles in water is 21×10^{-5} and with addition of 5, 10, 15 and 20 per cent particle volume fraction of Cu nanoparticle in water, thermal expansion got decreased to 19.9583×10^{-5} , 18.9167×10^{-5} , 17.8750×10^{-5} and 116.8334×10^{-5} , respectively represented in Figure 10. And height of percentage decrease of thermal expansion for 5, 10, 15 and 20 per cent gets comparatively increased for each stage from 4.96 to 5.22 to 5.50 to 5.83 per cent, respectively is represented in Figure 11(d). In case of CuO, thermal expansion for 0 per cent of particle volume fraction (i.e. pure base fluid) of CuO nanoparticles in water is 21×10^{-5} and with addition of 5, 10,

15 and 20 per cent particle volume fraction of CuO nanoparticle in water, thermal expansion got decreased to 19.9925×10^{-5} , 18.9850×10^{-5} , 17.9775×10^{-5} and 16.970×10^{-5} , respectively is represented in Figure 10. And height of percentage decrease of thermal expansion for 5, 10, 15, and 20 per cent gets comparatively increased for each stage from 4.80 to 5.04 to 5.30 to 5.60 per cent, respectively is represented in Figure 11(d). In case of SiO₂, thermal expansion for 0 per cent of particle volume fraction (pure base fluid) of SiO₂ nanoparticles in water is 21×10^{-5} and with addition of 5, 10, 15 and 20 per cent particle volume fraction of SiO₂ nanoparticle in water thermal expansion get decreased to 19.9525×10^{-5} , 18.905×10^{-5} , 17.85749×10^{-5} and 16.81×10^{-5} , respectively is represented in Figure 10. And height of percentage decrease of thermal expansion for 5, 10, 15, and 20 per cent gets comparatively increased for each stage from 4.99 to 5.25 to 5.54 to 5.86 per cent, respectively is represented in Figure 11(d). In case of TiO₂, thermal expansion for 0% of particle volume fraction (pure base fluid) of TiO₂ nanoparticles in water is 21×10^{-5} and with addition of 5, 10, 15 and 20 per cent particle volume fraction of Cu nanoparticle in water thermal expansion get decreased to 19.95459×10^{-5} , 18.9092×10^{-5} , 17.86379×10^{-5} and 16.8184×10^{-5} , respectively is represented in Figure 10. And height of percentage decrease of thermal expansion for 5, 10, 15 and 20 per cent gets comparatively increased for each stage from 4.98 to 5.24 to 5.53 to 5.85 per cent, respectively is represented in Figure 11(d).

Conclusion

The paper presents a new-fangled methodology to heat transfer mechanism to combine all the design aspects together for breeding a beneficial form of solution. This procedure is basically cooperative for R&D specialists to accept the design at the conceptual stage by considering all the design parameters concurrently. Designing a composite product keeping numerous aspects of design like environment, quality, reliability, cost, manufacturability, maintainability, etc., is a very immense assignment to the designer. The present paper proposes a new mathematical model, which consider all design aspects in a unified systems approach without trailing any valuable information. The model also has the capability to consider the interdependence of one design aspect over the other with the help of the design parameters. Since the model is derived from the matrix algebra, it is very convenient to store and to develop a software coding:

- (1) Concurrent design methodology for design of nanofluid used in heat exchanger for x-abilities using MADM approach provide a procedure for relative ranking of available nanofluids for a particular application.
- (2) Fishbone diagrams of various x-abilities are developed to identify all the attributes responsible for the cause while using nanofluid in heat exchanger. An exhaustive list attributes is developed via fishbone diagram that directly or indirectly affects performance of nanofluid for a particular application that assist to subside design time significantly.
- (3) This database of attributes is helpful to identify attributes responsible for optimum selection of nanofluid for a particular application thereby saving time of user and manufacturers.
- (4) Nature of variation of density, heat capacity, thermal conductivity and thermal expansion with varying particle volume fraction in sensitivity analysis is assisted by different graphs to demonstration percentage variation of pertinent attributes and it is noticed that all the selected nanofluids exhibit analogous

- property of constant degradation or upgradation of height of variation of pertinent attributes with varying particle volume fraction.
- (5) n -digit attribute based on coding scheme of nanofluids in an useful database for taking decisions. Database may contain un-normalised, normalised or weighted normalised attribute-based specification of nanofluids.
 - (6) The method converts large number of attributes into single numerical index for easy evaluation, comparison and ranking by decision makers.
 - (7) A MATLAB programming is established to execute calculations involved in the procedure.

References

- Ahmed, M.A., Shuaib, N.H. and Yusoff, M.Z. (2012), "Numerical investigations on the heat transfer enhancement in a wavy channel using nanofluid", *International Journal of Heat and Mass Transfer*, Vol. 55 Nos 21-22, pp. 5891-5898, available at: www.sciencedirect.com/science/article/pii/S0017931012004176
- Bhave, P., Narasimhan, A. and Rees, D.A.S. (2006), "Natural convection heat transfer enhancement using adiabatic block: optimal block size and Prandtl number effect", *International Journal of Heat and Mass Transfer*, Vol. 49 Nos 21-22, pp. 3807-3818, available at: www.sciencedirect.com/science/article/pii/S0017931006002924
- Choi, S.U.S. (1995), "Enhancing thermal conductivity of fluids with nanoparticles", *Developments and Applications of Non-Newtonian Flows*, FED-vol. 231/MD-vol. 66, ASME, New York, NY, pp. 99-105.
- Eastman, J.A., Phillpot, S.R., Choi, S.U.S. and Keblinski, P. (2004), "Thermal transport in nanofluids", *Annual Review of Materials Research*, Vol. 34, pp. 219-246, available at: www.annualreviews.org/doi/pdf/10.1146/annurev.matsci.34.052803.090621
- Eisher, W., Brunschweiler, T., Shalkevich, N., Shalkevich, A., Burgi, T., Michel, B. and Poulikakos, D. (2011), "On the cooling of electronics with nanofluids", *Journal of Heat Transfer*, Vol. 133 No. 5, , 11pp., available at: <http://heattransfer.asmedigitalcollection.asme.org/article.aspx?articleid=1449535>
- Hamilton, R.L. and Crosser, O.K. (1962), "Thermal conductivity of heterogeneous two-component system", *Industrial and Engineering Chemistry Fundamentals*, Vol. 1 No. 3, pp. 187-191, available at: <http://pubs.acs.org/doi/abs/10.1021/i160003a005>
- Heidary, H. and Kermani, M.J. (2012), "Heat transfer enhancement in a channel with block(s) effect and utilizing nanofluid", *International Journal of Thermal Science*, Vol. 57, pp. 163-171, available at: www.sciencedirect.com/science/article/pii/S1290072912000464
- Keblinski, P., Phillpot, S.R., Choi, S.U.S. and Eastman, J.A. (2002), "Mechanisms of heat flow in a suspension of nano-sized particles (nanofluids)", *International Journal of Heat and Mass Transfer*, Vol. 45 No. 4, pp. 855-863, available at: www.sciencedirect.com/science/article/pii/S0017931001001752
- Mahmoodi, M. and Hashemi, S.M. (2012), "Numerical study of natural convection of nanofluid in C-shaped enclosures", *International Journal of Thermal Science*, Vol. 55, pp. 76-89, available at: www.sciencedirect.com/science/article/pii/S1290072912000166
- Maxwell, J.C. (1881), *A Treaties on Electricity and Magnetism*, Vol. 1, 2nd ed., Clarendon Press, Oxford.
- Peyghambarzadeh, S.M., Hashemabadi, S.H., Hoseini, S.M. and Jamnani, M.S. (2011), "Experimental study of heat transfer enhancement using water/ethylene glycol based nanofluids as a new coolant for car radiator", *International Communications in Heat and Mass Transfer*, Vol. 38 No. 9, pp. 1283-1290, available at: www.sciencedirect.com/science/article/pii/S073519331100159X

- Singh, T. and Agrawal, V.P. (2012), "Concurrent design of nanoactuator for 'X-abilities' using the multiple-attribute decision-making approach", *Concurrent Engineering: Research and Applications*, Vol. 20 No. 4, pp. 301-314.
- Sui, Y., Lee, P.S. and Teo, C.J. (2011), "An experimental study of flow friction and heat transfer in wavy microchannels with rectangular cross section", *International Journal of Thermal Sciences*, Vol. 50 No. 12, pp. 2473-2482, available at: www.sciencedirect.com/science/article/pii/S1290072911002043
- Taylor, R., Coulombe, S., Otanicar, T., Phelan, P., Gunawan, A., Wei, Lv, Rosengarten, G., Prasher, R. and Tyagi, H. (2012), "Critical review of the novel applications and uses of nanofluid", *3rd Micro/Nanoscale Heat and Mass Transfer International Conference, Atlanta, GA 3-6 March*, pp. 219-234, available at: <http://proceedings.asmedigitalcollection.asme.org/proceeding.aspx?articleid=1715986>
- Wong, K.V. and De Leon, O. (2010), "Applications of nanofluids: current and future", *Advances in Mechanical Engineering*, Vol. 2, 11pp. doi: 10.1155/2010/519659, available at: <http://ade.sagepub.com/content/2/5/19659.full>
- Yu, W. and Choi, S.U.S. (2003), "The role of interfacial layer in the enhanced thermal conductivity of nanofluids: a renovated Maxwell model", *Journal of Nanoparticle Research*, Vol. 5 No. 1, pp. 167-171, available at: <http://link.springer.com/article/10.1023/A:1024438603801>
- Yu, W. and Xie, H. (2012), "A review on nanofluids: preparation, stability mechanisms, and applications", *Journal of Nanomaterials*, Vol. 2012, Article No. 435873, 17pp. doi: 10.1155/2012/435873, available at: <http://dl.acm.org/citation.cfm?id=2070291>
- Zoubida Haddad, E., Abu-Nada, H.F. and Oztop, A.M. (2012), "Natural convection in nanofluids: are the thermophoresis and Brownian motion effects significant in nanofluid heat transfer enhancement?", *International Journal of Thermal Science*, Vol. 57, pp. 152-162, available at: www.sciencedirect.com/science/article/pii/S1290072912000397

Appendix

To save time of user, and to avoid calculation errors and to make easier calculation work programming of MATLAB is preferred to solve all the including mathematical effort. MATLAB programme developed requires to enter number of alternates being observed, number of pertinent attributes under observation, decision matrix and relative importance matrix and by running programme all the calculation work will be performed and final values will be displayed as output. The programme constructed to solve all the calculation work is:

```
n = input('no of alternates = ')
m = input('no of pertinent attributes = ')
D = input('enter decision matrix = ')
for j = 1:m
nn(j) = norm(D(:,j));
end
for i = 1:n
for j = 1:m
N(i,j) = D(i,j)/nn(j);
end
end
fprintf('normalised matrix = ')
N
A = input('enter relative imp matrix = ')
eigen_value = eig(A)
[V X] = eig(A)
V1 = V(:,1)
eigen_vector = V1/V(1,1)
```

```

fprintf('relative weight vector = ')
w = (eigen_vector/sum(eigen_vector))'
for i = 1:n
for j = 1:m
Q(i,j) = N(i,j)*w(j);
end
end
fprintf('nomalised weight matrix = ')
Q
fprintf('positive ideal solution = ')
SP = max(Q)
fprintf('negative ideal solution = ')
SN = min(Q)
sumP = 0;
sumL = 0;
for i = 1:n
sumP = 0;
sumL = 0;
for j = 1:m
sumP = (sumP+(Q(i,j)-max(Q(:,j))).^2);
sumL = (sumL+(Q(i,j)-min(Q(:,j))).^2);
end
PP(i) = sqrt(sumP);
LL(i) = sqrt(sumL);
end
fprintf('positive separation measures = ')
P = PP
fprintf('negative separation measures = ')
L = LL
fprintf('relative closeness to positive benchmark index = ')
C = L./(P+L)

```

About the authors

Jyoti Prakash has started his career in teaching and research field. He have successfully completed his BTech in Mechanical Engineering and ME in Thermal Engineering. For the partial fulfilment of his master degree he has completed his thesis under the guidance of Professor Dr V.P. Agrawal. Jyoti Prakash is the corresponding author and can be contacted at: l_tomar@yahoo.com

Vishnu P. Agrawal is working as a Visiting Professor in Mechanical Engineering Department at the Thapar University, Patiala, Punjab, India. He had been at IIT Delhi as a Senior Professor for the last 28 years in Mechanical Engineering Department. He completed his graduation in 1966 and post-graduation in 1969 and PhD in 1983 from the Jiwaji University Gwalior, University of Roorkee, and IIT Delhi, respectively. He has published around 150 papers in international journals and conferences. He has guided successfully a large number of BTech, ME projects, and supervised a number of PhD thesis. He has worked extensively in the areas of mechanisms, systems approach and machine design.

For instructions on how to order reprints of this article, please visit our website:

www.emeraldgroupublishing.com/licensing/reprints.htm

Or contact us for further details: permissions@emeraldinsight.com